ELSEVIER

Fusion Engineering and Design 39–40 (1998) 759–764

Fusion Engineering and Design

Mechanical behavior and design database of packed beds for blanket designs

Alice Y. Ying *, Zi Lu, Mohamed A. Abdou

Mechanical and Aerospace Engineering Department, University of California, Los Angeles, CA 90095-1597, USA

Abstract

The mechanical behavior and properties of particle beds relevant to fusion ceramic breeder blanket designs are addressed through a combination of experimental and analytical studies. A series of uniaxial compression tests are performed in a INSTRON hydraulic-press test facility in which compressive loads are applied to Li_2ZrO_3 and aluminum packed beds. The experimental data shows that the mechanical properties such as the bed effective modulus are stress dependent and consistent with the analytical model predictions. Nevertheless, the experimental data shows that the bed effective modulus is approximately two orders of magnitude lower than that of the solid material.

1. Introduction

From a structural viewpoint, particle beds are composed of mutually contacting solid particles, or structural units. The existence of the contacts restrict the freedom of motion of the individual particles, and thus, conditions the strength and the rigidity of the bed. The mechanical properties of the bed approach those of solids, or of gases depending upon the strength of the structural units, the nature of the interaction between the various phases, the state of the particulate material in question, etc. Once the bed is loaded, the load propagates through the particles via the finite number of contacts. Due to the comparatively low strength of the bonds between the particles, the structure of the particle bed changes, i.e. irreversible deformations takes place even at low values of stress. It is the friction bond that is the principal difference in the mechanics between particulate and continuous medium, and is an immediate result of the restricted freedom of motion of the particles.

The mechanical properties of the packed beds of interest to fusion blanket design include Young's (effective) modulus, equivalent Poisson ratio, and the inter-particle coefficient of friction. The effective modulus and equivalent Poisson's ratio are needed to predict the induced stress exerted on the clad/bed due to the differential expansion from thermal or radiation induced swelling. Moreover, those induced mechanical stresses are known to alter inter-particle contact characteristics and consequently the thermal performance of the packed bed. The available commercial finite element thermomechanical analysis codes, such as ANSYS, cannot correctly predict the thermomechanical performance of a packed

* Corresponding author.

0920-3796/98/$19.00
PII S0920-3796(97)00157-9

bed without knowing the magnitudes of the aforementioned mechanical properties and the nature of the bed mechanical behavior. Also, it is likely that undesirable voids might be formed during operation due to the degradation or breakage of the pebbles. Thus, it is important to know to what degree particles would flow by gravitation or other active forces to fill the voids. In order to be able to adequately predict blanket thermal mechanical performance, experimental investigations of mechanical force in packed beds relevant to fusion solid breeder blanket designs need to be performed. In this paper, the mechanical behavior of packed beds under external loads and experimental data concerning mechanical properties such as the effective moduli and Poisson's ratios are presented and compared with the available analytical studies.

2. Definition of structural mechanical properties of particle bed

The effective modulus of the particle bed is determined from the relationship between the average incremental stress and the average incremental strain of the packing after an initial deformation. The effective moduli, C_{ijkl}, is defined by the following equation:

$$\langle \delta\sigma_{ij} \rangle = C_{ijkl} \langle \delta\varepsilon_{kl} \rangle \tag{1}$$

where $\langle \delta\sigma_{ij} \rangle$ is the average incremental stress, $\langle \delta\varepsilon_{kl} \rangle$ the average incremental strain, and i, j, k, $l = 1, 2, 3$.

If the bed is undergoing hydrostatic compression, the effective moduli can be expressed in terms of the effective Lame constants, λ^* and μ^*, as follows [1,2]:

$$C_{ijk_l} = \lambda^* \delta_{ij}\delta_{kl} + \mu^*(\delta_{ik}\delta_{jk} + \delta_{il}\delta_{jk}) \tag{2}$$

where Kronecker $\delta_{ij} = 1$ for $i = j; = 0$ for $i \neq j$, and

$$\lambda^* = \frac{(1-\phi)}{20\pi}\left\{\frac{\eta_0}{R}\,(D_N(\phi) - D_T(\phi))\right\} \tag{3}$$

and

$$\mu^* = \frac{(1-\phi)}{20\pi}\left\{\frac{\eta_0}{R}\,(D_N(\phi) + \tfrac{3}{2}\,D_T(\phi))\right\} \tag{4}$$

D_N and D_T are the normal and tangential contact stiffness, respectively. They are defined as:

$$D_N = \frac{dF_N}{dw} \tag{5}$$

and

$$D_T = \frac{dF_T}{dr} \tag{6}$$

where dF_N and dF_T are the magnitude of the normal and tangential component of the incremental contact force, respectively, dw is the incremental normal component of the displacement, and dr is the incremental tangential component of the displacement.

The Poisson's ratio (v^*) under the hydrostatic condition is defined as:

$$v^* = \frac{\lambda^*}{2(\lambda^* + \mu^*)} \tag{7}$$

From Eqs. (2)–(4), and Eq. (7), it can be seen that the magnitude of the effective bed mechanical properties are functions of the bed characteristics described by the porosity (ϕ), particle radius (R), the number of contacts per particle (η_0), and of the contact stiffness $D_N(\phi)$ and $D_T(\phi)$.

3. Test apparatus

The principle part of the test apparatus, shown in Fig. 1, includes a cylindrical test particle bed (with an inner bed diameter of 5.17 cm and an experimental height up to 21 cm) loaded with a vertical axial pressure provided by a hydraulic press (INSTRON hydraulic stress strain test facility) and measured by a load cell. The axial displacement of the bed is measured by a transducer, while the radial strains along the axial direction are measured through a set of strain gauges. In addition, a pressure transducer is installed on the side of the test article for measuring the corresponding radial stress. The experiments were performed for Li_2ZrO_3 ceramic beds (particle size of ≈ 1–1.2 mm diameter) and aluminum particle beds (with particle diameter of 0.5 mm) and the

process involved a uniaxial compressive deformation. During the compression, the mobile particles press/slide against one another which reduces the porosity of the bed. It is important to note that the uniaxial compression implies an anistropic response and that the test results only reflect those properties in the principal stress direction.

4. Test results and the derivation of mechanical properties

The axial compressive strain versus the axial compressive stress during loading and unloading conditions are shown in Figs. 2 and 3 for Li_2ZrO_3 and aluminum packed beds, respectively, in which the compressive stress is calculated as the applied force over the bed cross sectional area while the compressive strain is calculated as the incremental packing density over the initial packing density. The steep gradient found in the relationship between the stress and axial compressive strain under subsequent loading conditions indicate that the deformation of the particle bed is largely a consequence of the displacements of the particles and is irreversible. These irreversible deformations are indicative of changes of state and they make it

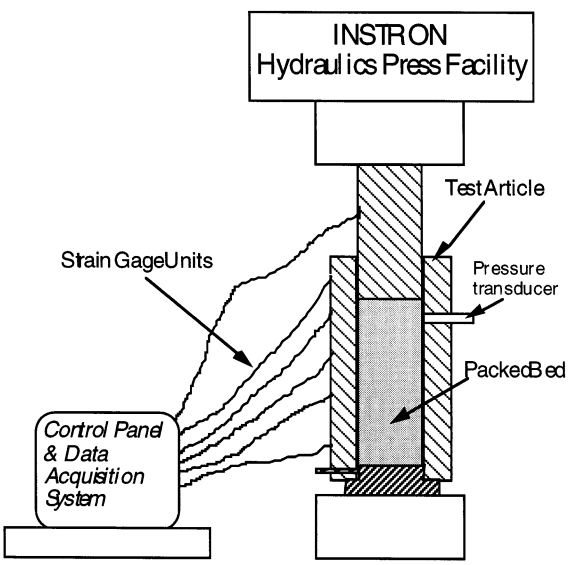

Fig. 1. Uniaxial compression test facility.

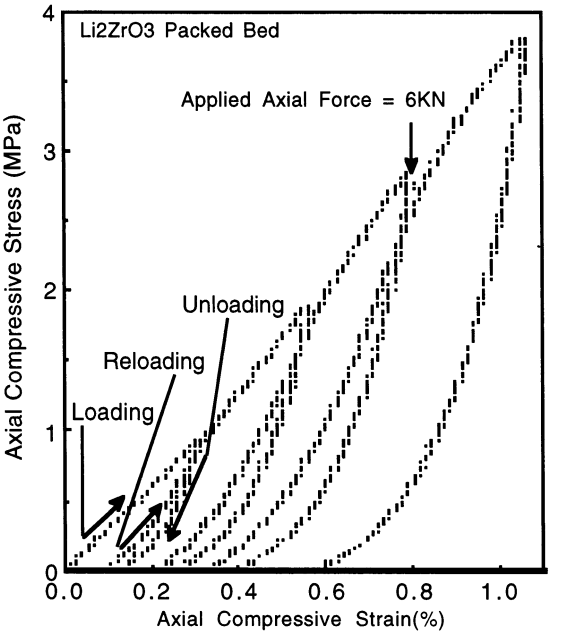

Fig. 2. Stress vs. strain during cyclic loading and unloading tests (initial bed packing density = 57.5%).

imperative to redefine the mechanical behavior on the basis of state quantities. During the course of the loading and unloading experiments on the ceramic packed bed as shown in Fig. 2, a sudden change in the slope of the stress and strain curve found at the applied force of ≈ 6 KN (equivalent to 2.85 MPa) intimates a change of the bed structure. Post-test examination of the bed reveals that those ceramic particles near the location where the force is applied are crushed; in the middle of the bed, particles become interlocked, while the state of the particles at the bottom of the bed remained the same. This suggests that the applied force is offset by the frictional forces as it is transmitted to the bottom of the bed. For the aluminum particle beds, inter-particle locking was discovered at an external pressure of ≈ 70 MPa.

The calculated uniaxial modulus of deformation, E_a, after prestraining in compression, as a function of continued further loading, σ_a, are shown in Fig. 4. As is seen, the effective modulus in the axial direction increases with an increase in the axial stress. This indicates that E_a for a particular material depends essentially on the principal

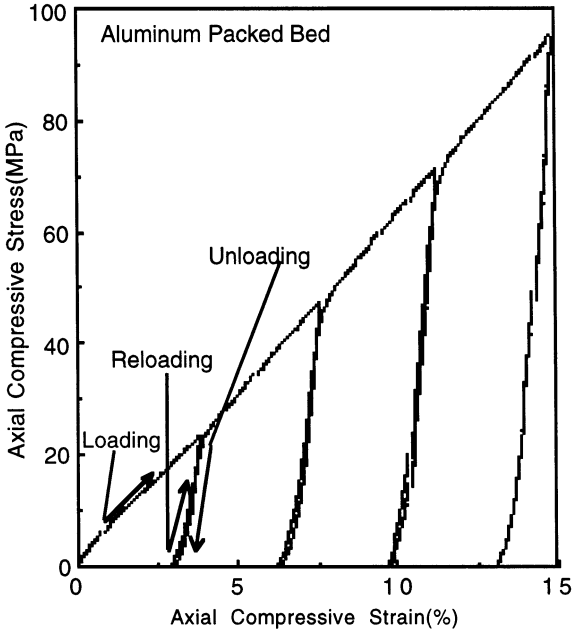

Fig. 3. Stress vs. strain during cyclic loading and unloading tests (initial bed packing desnsity = 59.0%).

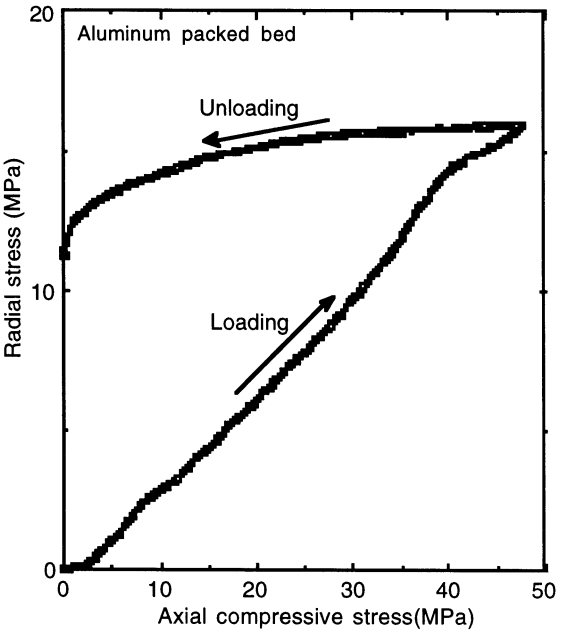

Fig. 5. Radial local stress vs. axial local stress (at top of the bed) during loading and unloading of aluminum packed bed.

stress in the direction of the major strain increment for which the E_a value is defined. For an arbitrary compressibility curve, the stress and strain relationship can be modeled as [3]:

$$E_0 = \frac{1}{c}\sigma_a^m \tag{8}$$

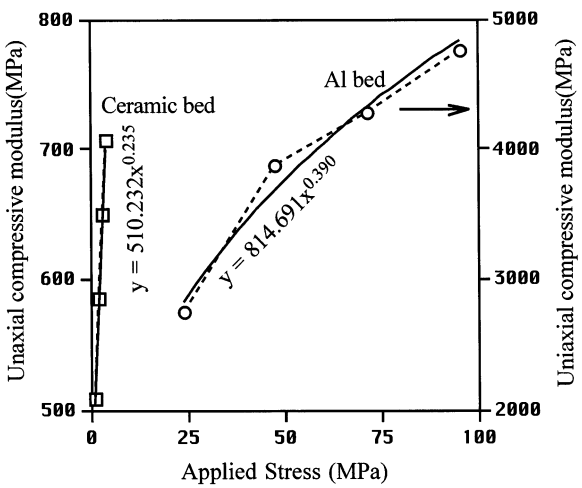

Fig. 4. Compressive modulus as a function of applied stress.

where c is the coefficient of compressibility, and m is the exponent expressing the intensity of the structural changes. The estimated values of c and m and the corresponding curves are also shown in Fig. 4. The correlation shows that the aluminum packed bed has a smaller degree of compressibility yet a stronger intensive structural change compared to the ceramic bed.

The relationships between axial stress and horizontal stress for the aluminum particle bed during loading and unloading are shown in Fig. 5. For a deterministic set of spheres, one can calculate the coefficient of lateral pressure (K_0) by [3]:

$$K_0 = \frac{\sigma_r}{\sigma_a} \tag{9}$$

The result shown in Fig. 5 indicates that throughout the deformation process K_0 is a constant, and that for uniaxial loading this constant can be expressed as:

$$K_0 = \frac{1}{2}\frac{1-f}{1+f} \tag{10}$$

where f is the coefficient of friction on the sliding surface of the two particles. The calculated coefficient of lateral pressure and coefficient of friction for the aluminum packed beds are 0.339 and 0.192, respectively. The magnitude of f determines the magnitude of the tangential component of the contact force (T), at the onset of particle slide through $T = fP$, where P is the normal component of the contact force. In this sense, f expresses the bed's resistance to its rearrangement.

As the effect of skin and inter-particle friction, the axial stress of the sample decreases with increasing depth. This phenomena plotted for the aluminum packed bed is shown in Fig. 6. For a decrease in the vertical pressure σ_a where the depth (h) is measured from the value of σ_{max}, an experimental relation was derived [3]:

$$\sigma_a = \sigma_{max} \exp\left(m_b \frac{h}{R_b}\right) \tag{11}$$

where R_b is the ratio between the cross-sectional area and the perimeter of the test bed and m_b is the product of K_0 and the coefficient of skin friction. The experimental values of m_b were estimated based on the pressure transducer measurements along the direction of the applied force. The calculation gives a value of 0.106 for the aluminum packed bed as shown in Fig. 6. A higher value of 0.399 is found for the Li_2ZrO_3 ceramic packed bed which is consistent with the numbers reported for hard ceramic powders which range between 0.35 and 0.45. This indicates that the idea of using an external force to re-direct the particle bed packing arrangement will not be effective if the skin friction and interparticle friction are significant. The designer has to warrant that a perfect contact could be maintained passively along the breeder/multiplier and cladding interface, especially in design cases where particle fragmentation would lead to the formation of a void perpendicular to the direction of heat flow.

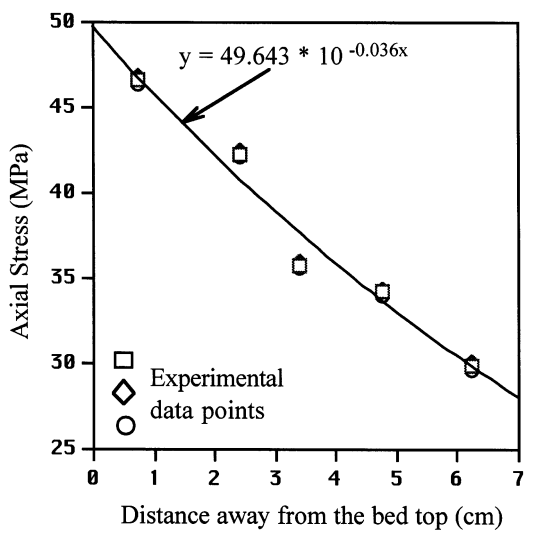

Fig. 6. Axial local stress as a function of distance away from the bed top (aluminum packed bed).

The Poisson's ratio can be calculated by assigning the value of zero to the bed radial strain, which gives:

$$\nu_a = \frac{\sigma_r}{\sigma_a + \sigma_r} = \frac{K_0}{1 + K_0} \tag{12}$$

The calculated Poisson's ratio for the aluminum packed bed is equal to 0.253 which is close to the theoretical value of 0.25 for a perfectly smooth sphere packed bed.

5. Comparison with the available analytical model

The effective modulus in the principal stress direction of a random-dense packing under an uniaxial compression has been derived theoretically for both infinitely rough and perfectly smooth spheres [1]:

$$C_{33} = 8(\alpha + \beta) \text{ for infinitely rough sphere, and} \tag{13}$$

$$C_{33} = 3\alpha \text{ for perfectly smooth sphere} \tag{14}$$

where

$$\alpha = \frac{(1-\phi)\eta_0(-e_a)^{1/2}}{32\pi^2 B} \text{ and } \beta = \frac{(1-\phi)\eta_0(-e_a)^{1/2}}{32\pi^2(2B+C)} \tag{15}$$

$$B = \frac{1}{4\pi}\left\{\frac{1}{\mu} + \frac{1}{\lambda+\mu}\right\} \text{ and } C = \frac{1}{4\pi}\left\{\frac{1}{\mu} - \frac{1}{\lambda+\mu}\right\} \tag{16}$$

λ and μ denote the Lame moduli for the sphere material and e_a is the magnitude of the uniaxial compression. Fig. 7 shows the calculated effective modulus as a function of axial compressive strain

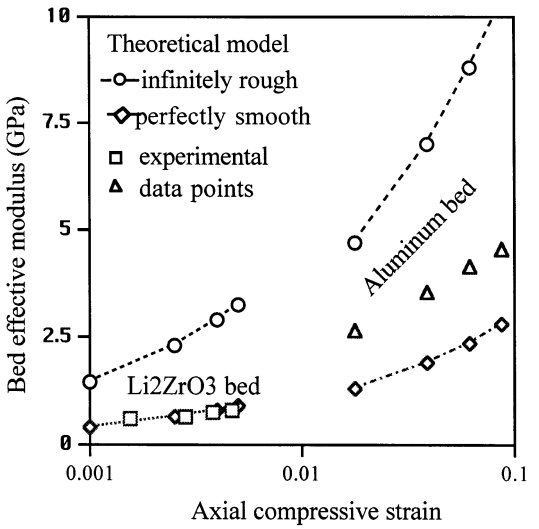

Fig. 7. Comparison of experimental data of effective modulus with theoretical curves.

and compared with the experimental values of aluminum and Li_2ZrO_3 packed beds. The experimental results fall between these two extremes and tends toward the smooth sphere condition for both ceramic and aluminum particle beds examined.

6. Conclusions

The mechanical properties of packed beds were experimentally studied and compared with available theoretical solutions. The experimental results show that the stress–strain relation for cyclical loading depends on the loading history. Nevertheless, the experimental data shows that the bed effective modulus is approximately two orders of magnitude lower than that of the solid material. The undisturbed state of the particles found at the bottom of the ceramic packed bed illustrates the important role that micro-scale mechanical properties play on the macro-scale behavior. The degrees of freedom of particle motion are hindered by inter-particle friction and skin friction. This is consistent with the experimental observations where no indication of small broken particles had settled down to the bed bottom [4]. Available theoretical studies reveal that the mechanical characteristics at the microscopic level is complex. The effective modulus of a packed bed is significantly dependent upon the inter-particle contact stiffness and the geometric arrangement. Due to the macro-scale bed behavior being largely influenced by the micro-scale mechanical properties, further experimental research in this area is warranted.

Acknowledgements

This work was performed under the US Department of Energy Contract DE-F603 86ER52123.

References

[1] K. Walton, The effective elastic modulus of a random packing of sphere, J. Mech. Phys. Solids 35 (2) (1987) 213–226.
[2] A.L. Endres, The effect of contact generation on the elastic properties of a granular medium, Trans. ASME 57 (1990) 330–336.
[3] J. Feda, Mechanics of Particulate Materials, The Principles, Elsevier Scientific, chps. 1, 4, and 5 (1982).
[4] P. Gierszewski, M. Dalle Donne, H. Kawamura, M. Tillack, Ceramic pebble bed development for fusion blankets, Fusion Eng. Des. 27 (1995) 167.